Astron. Astrophys. 316, 296–303 (1996)

ASTRONOMY
AND
ASTROPHYSICS

Ulysses plasma parameters: latitudinal, radial, and temporal variations

B.E. Goldstein[1], **M. Neugebauer**[1], **J.L. Phillips**[2], **S. Bame**[2], **J.T. Gosling**[2], **D. McComas**[2], **Y.-M. Wang**[3], **N.R. Sheeley**[3], **and S.T. Suess**[4]

[1] Jet Propulsion Laboratory, California Institute of Technology, Pasadena, CA, 91109, USA
[2] Los Alamos National Laboratory, Los Alamos, NM 87545, USA
[3] Naval Research Laboratory, Washington, DC 20375, USA
[4] NASA/Marshall Space Flight Center, Huntsville, Alabama 35801, USA

Received 26 February 1996 / Accepted 29 August 1996

Abstract. Observations by the Ulysses SWOOPS plasma experiment are used to investigate spatial and temporal gradients during the mission, with emphasis on more recent high latitude observations including the recent South Pole to North Pole passage during solar minimum. Compared to lower latitudes, the high latitude solar wind had higher average speed, proton temperature, and momentum flux, and lower number flux density. As the average momentum flux observed in the high speed wind was 21% greater than at the equator, during solar minimum the distance to the heliopause will be comparatively less in the solar equatorial plane than over the poles. The long term temporal gradients of momentum flux over the life of the mission are considerably larger than the latitudinal gradient observed by Ulysses during solar minimum. A modest North-South high latitude asymmetry is observed in the plasma parameters; the velocity is on the average 13 km/s to 24 km/s greater at Northern latitudes than at Southern, and temperature is also higher. The North-South temperature asymmetry is greater than can be explained by the North-South velocity difference and the dependence of solar wind temperature upon speed. The power law dependence of temperature on heliocentric distance, r, at high latitudes is in range $r^{-0.81\mathrm{to}-1.03}$, where $r^{-0.81}$ is the Southern latitude result and $r^{-1.03}$ the Northern. The parameter $T/n^{1/2}$, where T is temperature and n is proton number density, can be better predicted from speed than can temperature alone. Comparison with calculations based on source models and magnetograph data indicate that the expansion of open coronal field lines close to the Sun was greater in the Southern hemisphere than in the Northern; this anticorrelation with the expansion factor is consistent with previous observational and theoretical work.

Key words: Sun: solar wind – interplanetary medium

Send offprint requests to: B.E. Goldstein
(bgoldstein@jplsp2.jpl.nasa.gov)

1. Introduction

We report on solar wind proton observations of the Ulysses SWOOPS plasma experiment (Bame et al. 1992) obtained at high heliographic latitudes and during the recent passage from high Southern to high Northern latitudes. The Ulysses spacecraft was launched in October of 1990, encountered Jupiter in February of 1992, and was deflected at Jupiter encounter towards high Southern latitudes. The Southern-most latitude of -80°was reached September 13, 1994; Ulysses crossed the heliographic equator on March 4 of 1995, and reached highest Northern latitudes of 80°on July 31, 1995. The measurements obtained during the rapid latitude traversal from -80°to 80°(referred to herein as the fast latitude scan) are a primary topic of investigation of this paper. Since the fast latitude scan occurred during the minimum of the solar cycle when the current sheet is close to the equator, clear and systematic differences between the high latitude and low latitude observations are apparent that might not be seen at other times in the solar cycle. The variation with latitude of solar wind speed, number flux, momentum flux, and temperature are investigated as a function of latitude during the fast latitude scan; for the purposes of comparison we have also investigated radial and solar cycle behaviors of these parameters as needed.

2. South-to-north polar pass: overview

An overview of the South to North fast latitude scan data is provided as 12 hour averages in Fig. 1. This interval has been previously discussed (Phillips et al. 1995) in a study of latitudinal gradients, in terms of coronal sources (Gosling et al. 1995), and dynamical stream interactions (Gosling et al. 1995). Shown in a stacked panel plot as a function of heliographic latitude for the period of the South to North polar pass are various parameters: a) Uppermost panel shows solar wind speed, b) scaled momentum flux in units of 10^8 dynes cm^{-2}AU^2, c) scaled proton density in cm^{-3}AU^2, d) scaled proton number flux in units

of $10^5 cm^{-2}s^{-1}AU^2$, and e) ion temperature in K (dashed line), and distance, r, of Ulysses from the Sun in AU, solid line. The parameters in b,c,d have all been scaled to 1 AU by multiplication by r^2. The variable plotted as temperature in Fig. 1e is in fact the radial component of the temperature tensor for reasons discussed in the section below on temperature gradients. Several features are of interest. First, the entrance to and exit from the low latitude streamer belt is quite abrupt. At high latitudes, speed is high and density is low, similar to what is observed in high speed solar wind streams at low latitudes. Ascending in latitude from the South pole, at -38.5°latitude Ulysses first encountered low speed solar wind associated with the Southernmost extension of the streamer belt. Following this brief observation of slow plasma, Ulysses remained in the high latitude solar wind until about -22°, at which point there was a forward shock, a coronal mass ejection (CME) was encountered, and Ulysses was thereafter in low speed streamer belt plasma. In the streamer belt, the velocity was much lower. The density is most strongly anticorrelated with the velocity and temperature (compare Fig. 1a and 1e with 1c), whereas the variable that is most constant across all latitudes when averaged over solar rotations is the proton momentum flux (Fig. 1d); many previous workers have noted the constancy of momentum flux within the ecliptic plane (e.g., Schwenn 1990). Note that for all variables in the low latitude solar wind there are large increases associated with interaction regions. For further information on the dynamics and sources within this region see the Gosling et al. references; additionally, information on the current sheet location discussed by Smith et al.(1995).

3. Latitudinal momentum flux variations

To investigate further the properties of momentum flux, we have plotted in Fig. 2 averages (solid line) and medians (dashed line) over 4°latitude bins of the solar wind momentum flux during the fast latitude scan. If one examines the momentum flux during the South to North Pole passage, a significant decrease of the momentum flux between -20°to +20°latitude is observed. This is the same data 4°averaged presented in Fig. 2 of Phillips et al. (1995). Fig. 3 of Phillips et al. (1995) shows a postulated shape of the heliosphere based on median values of the solar wind momentum flux; however, the average location of the heliopause is presumably determined by the average momentum flux rather than the median (stream collisions further from the Sun form merged interaction regions which further complicate the issue). Because the interaction regions in low latitude solar wind typically have large increases in solar wind parameters for a relatively small fraction of the time, averages will be somewhat larger than medians. The data in Fig. 1 indicate that, although the latitudinal variation of the average momentum flux is less than that of the mean, the conclusion of Phillips et al.(1995) that the termination shock should, during solar minimum, be elongated in the polar direction (i.e., "peanut shaped") is still supported, although the effect is somewhat less pronounced than originally suggested. The high latitude (greater than 20°) average momen-

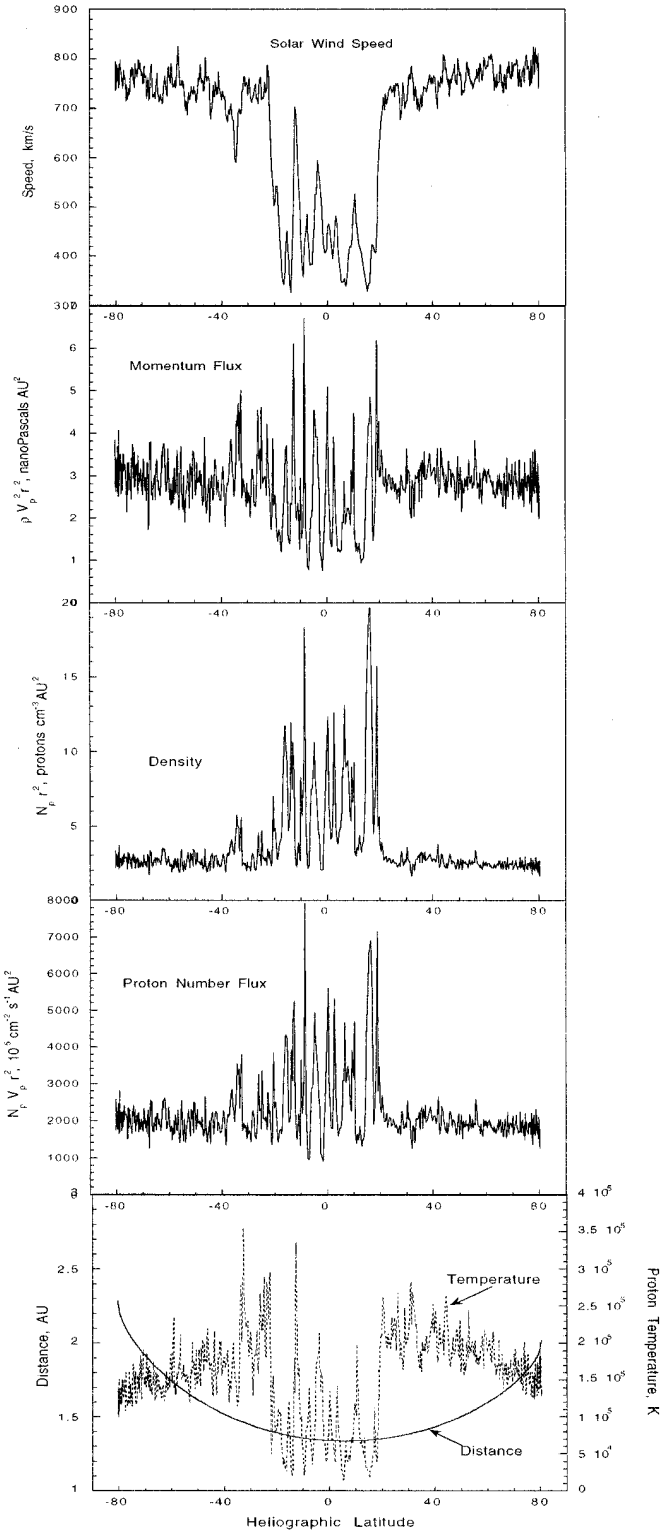

Fig. 1. Ulysses plasma parameters during the fast latitude scan

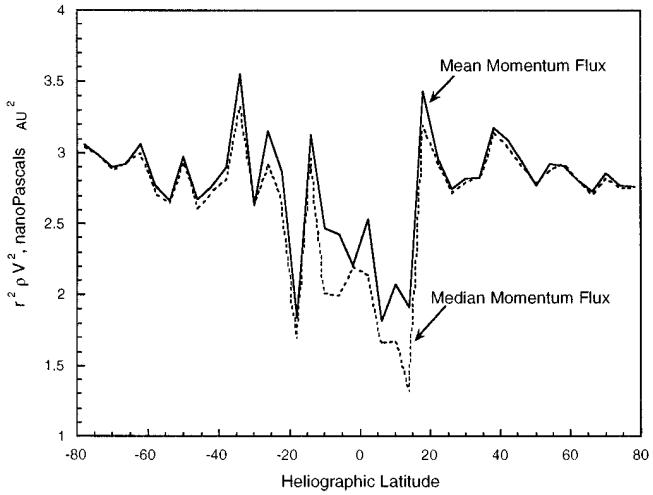

Fig. 2. Median and average momentum flux

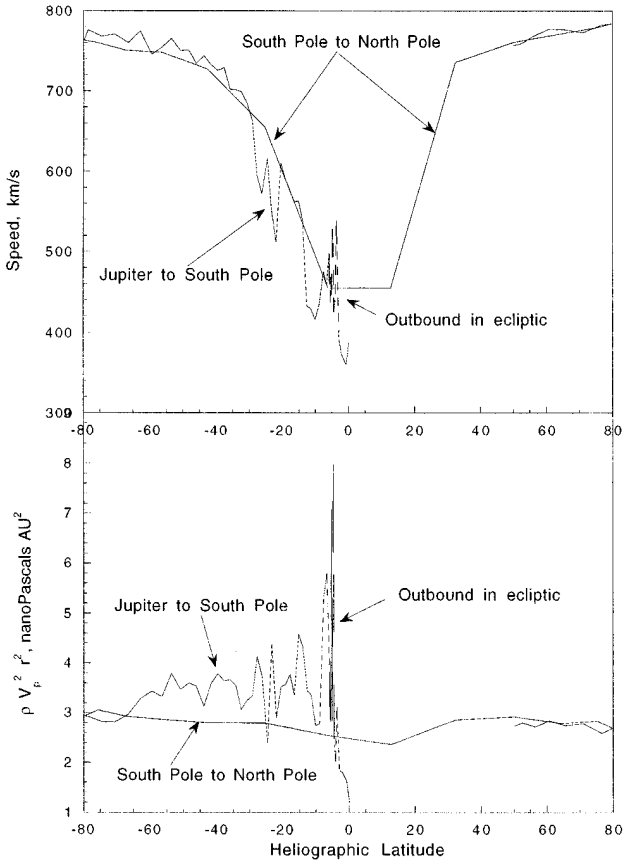

Fig. 3. Speed and scaled momentum flux as functions of heliographic latitude

tum flux is about 2.9 nanoPascals (nP), whereas the low latitude flux (less than 20°) is 2.4 nP.

To determine to what extent the momentum fluxes might be time variations, and to what extent the variations are dependent on solar cycle, in Fig. 3 we have plotted averages over Carrington rotations of solar wind speed and scaled momentum flux as a function of heliographic latitude all the data obtained by Ulysses since Day 351 of 1990. The momentum flux is shown in the lower panel and the speed in the upper panel. Ulysses initially traveled outwards from the Sun in the ecliptic, resulting in the large amount of data just south of the heliographic equator. After Jupiter encounter, Ulysses began a slow rise to high Southern latitudes, the data from this period are more closely spaced in latitude than those during the fast latitude scan. Examination of the data shows the dip in momentum flux during the South-North fast latitude scan. It can be seen that during the Jupiter to South pole phase the momentum flux was greater at the same latitude than during the South to North pole pass. The variation of speed and momentum flux near the ecliptic plane are not shown well in the format of Fig. 3, so a separate plot showing momentum flux and heliographic latitude as a function of time is shown in Fig. 4. As Ulysses provides essentially continuous data coverage, the significant variability from rotation to rotation of the momentum flux during 1991 and 1992 is presumably the result of CMEs interacting with the solar wind . It is difficult to define a typical value of the momentum flux during the outbound to Jupiter phase of the mission, values as low as 2 nP might be assigned based on the data obtained from 1.5 to 2.5 AU (prior to March 25, 1991), whereas if one looks at data obtained beyond 2.5 AU, estimates might be in the range 3.5-4 nP. Lazarus and McNutt (1990) have used Voyager data obtained in the ecliptic from 1978 through 1989 to determine the solar cycle variation of the momentum flux. They find that during 1983 to 1985, 11 years prior to the Ulysses fast latitude scan passage through the ecliptic in early 1995, typical momenta fluxes were about 3.5 nP. During the more active portion of the solar cycle momentum fluxes were observed to be lower; for example from 1979 through 1981 the value was about 2.2 nP, and their latest data (1988 through about 1989.3) indicate a value of about 2.5 nP. For reference, Feynman et al.(1993) find the peaks of the last three solar cycles to occur in 1968.9, 1979.9, and 1989.9, with the last peak being rather broad. Schwenn (1990) finds that the momentum flux is modulated by $\pm 28\%$, with the peak coming two years after the activity maximum. The Ulysses data show that the general trend of largest momentum fluxes occurring during the declining portion of the solar cycle holds true in the present solar cycle. Additionally, comparing the temporal variations in momentum fluxes with the dip as the equator was crossed in early 1995, it is apparent that although the heliosphere should be somewhat more extended in the polar direction than the equatorial (peanut shape) at solar minimum, there are major long term variations of momentum flux over the solar cycle with big peaks due to CMEs.

4. Speed variations: north-south asymmetry, coronal expansion factor

A North-South asymmetry of the solar wind speed was observed during the fast latitude scan. Averages of speed over Carrington rotations are shown in Fig. 5 as a function of the absolute value of heliospheric latitude; also plotted is the coronal expansion factor averaged over a Carrington rotation at the latitude of

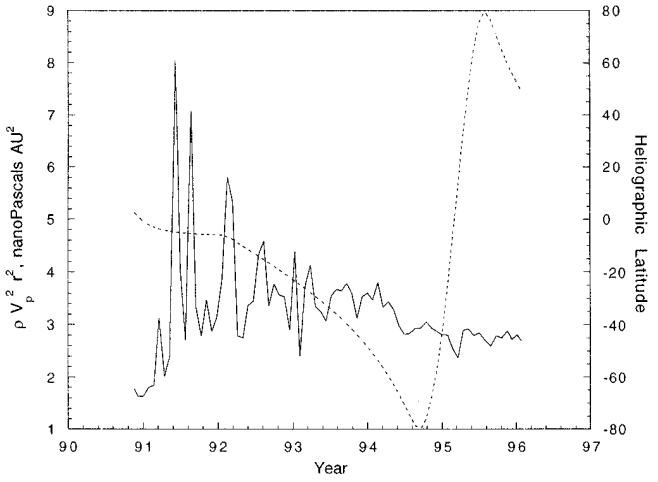

Fig. 4. Scaled momentum flux and heliographic latitude throughout the mission

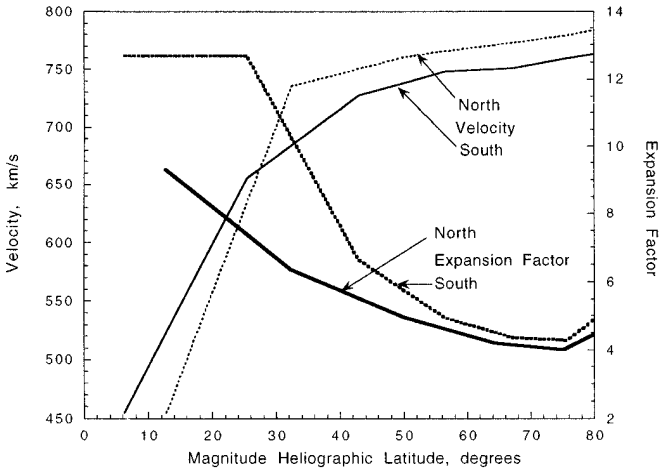

Fig. 5. Speed and coronal expansion factor for the Northern and Southern hemispheres

Ulysses. Expansion factor as used herein is defined as the factor by which a magnetic flux tube expands between the photosphere and 2.5 solar radii relative to r^2 expansion. Expansion factors were calculated as follows: magnetograph data from the Wilcox Solar Observatory were corrected for projection effects by assuming a radially oriented magnetic field. The radial magnetic field was used as a lower boundary condition for a potential solution in a spherical shell with inner radius at the photosphere and outer radius of 2.5 solar radii. Above 2.5 solar radii, for calculational purposes, the field is temporarily assumed to be all of the same polarity and satisfy a potential solution; to match the solutions above and below 2.5 solar radii the magnitude of the radial component of the magnetic field is required to be continuous across the surface at 2.5 solar radii. After the solution is obtained, the actual polarity of the field based on the sign of the radial field at the source surface is used in the outer region. The procedure of having flux of only one polarity above the source surface is equivalent to inserting a current sheet between regions of inward and outward flux at the Sun, and ensures that far from the Sun the flux depends only on distance from the Sun (i.e., no latitudinal or longitudinal variations). This method of assuming polarity reversal to obtain a potential solution with an embedded current sheet was first used by Schatten (1971), and is described elsewhere (Wang and Sheeley 1988) in more detail than here. It is clear that considerable assumptions are involved in such calculations, and the most robust method of estimating the expansion factor (and predicting the properties of the solar wind) would be an MHD calculation.

The data in Fig. 5 show that the speed in the Northern hemisphere at latitudes greater than 40°was typically about 15-20 km/s larger than the speed at comparable Southern latitudes. A least squares fit of 12 hour averages of solar wind speed (not shown) to latitude over the range 40°to 80°resulted in a velocity difference of 24 km/s at 40°decreasing to 13 km/s at 80°. Wang and Sheeley (1990) established an observational inverse correlation between the solar wind speed observed at 1 AU and the areal expansion factor in the inner corona as estimated from magnetograph data and modeling. The data shown in Fig. 5 do qualitatively agree with this inverse relationship. The expansion factor is lower (higher) at higher (lower) latitudes, and the velocity has the opposite behavior. Further, the high latitude expansion factor is lower in the North than in the South, and the velocity is higher in the North.

To determine how well this agrees with the full set of Ulysses observations we show in Fig. 6 a plot of expansion factor as a function of time for the entire mission. There is qualitative agreement with an inverse correlation between expansion factor and velocity. When Ulysses crossed the heliospheric equator in early 1995 the velocity was about 450 km/s and the expansion factor was estimated to be about 10 to 12. Earlier in the mission before leaving the ecliptic plane velocities of 450 km/s were also encountered, but the expansion factors during these times were about a factor of two larger than the early 1995 value. A significant distinction between the early 1995 and the earlier in-ecliptic data is that Ulysses was traveling rapidly in latitude, and the data are averaged over a rotation to remove longitudinal variations. Since the earlier data are more centered in the current sheet, and the expansion factor near the current sheet varies rapidly as a function of latitude in this region, it is possible that averaging the expansion factor over the actual trajectory rather than taking the average latitude for a particular rotation would have increased somewhat the expansion factor estimated for the central part of the early 1995 equatorial crossing. Also, note that the Ulysses data are averaged over mapped back Carrington longitudes from 0°to 360°, as are the expansion factors, but because of the longitudinal difference between Ulysses and the Earth the actual central time of the intervals can be different by up to half a solar rotation. This explains why the expansion factor values shown in Fig. 5 for the Southern hemisphere at -25°and -6°are equal; the Earth-spacecraft longitude difference crossed 180°.

Fig. 7 displays expansion factor as a function of solar wind speed. It can be seen that small values of the expansion factor (less than about 7) are excellent predictors of high solar wind

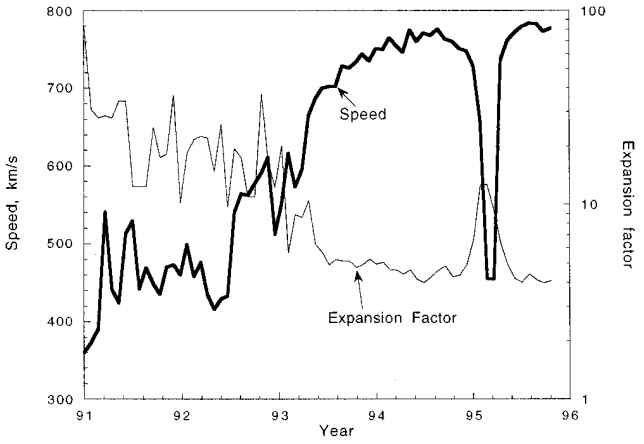

Fig. 6. Speed and Coronal Expansion Factor for the Ulysses Mission

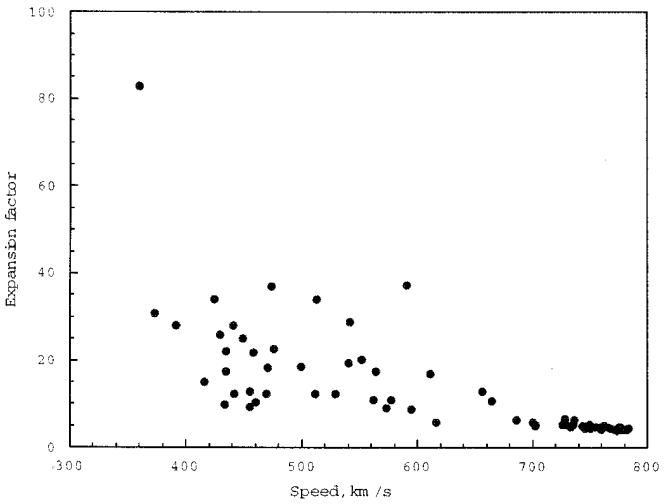

Fig. 7. Expansion factor as a function of speed

speeds (>600 km/s), but for larger expansion factors, although there is clearly a trend toward lower speeds, the correlation becomes much more scattered and expansion factor does not have much predictive value. Recent results (Wang et al. 1996) from in-ecliptic spacecraft measurements using daily averages also show the same general trend and considerable scatter (their Fig. 6c).

5. Latitudinal and radial temperature variations

It has long been known that temperature in the solar wind is typically correlated with the solar wind speed (Neugebauer and Snyder 1966), (Strong et al. 1966), and comparing Figs. 1a and 1e it is clear that this relationship holds for the fast latitude scan. Since it was found that the speed over the North pole was larger than over the South pole, one might expect a comparable relationship for temperature. However, Ulysses was closer to the Sun over the North pole than the South, and as solar wind temperature decreases with distance from the Sun further investigation is needed to determine whether this is a radial or a latitudinal gradient.

Some properties of the SWOOPS experiment and the ion temperature estimates are also significant. The energy resolution of the instrument is 2.5% ΔE/E for an energy step. Although individual spectra are taken in two step intervals, by combining temporally adjacent spectra an energy resolution of 2.5%, or 1.25% in velocity space, is obtained. For a solar wind beam traveling 750 km/s, and having a temperature of about 1.4 10^5K at 2 AU, the thermal speed is about 6.4% of the bulk speed. The temperature in the energy direction is therefore very well resolved, whereas in the angular direction our resolution is not as good, and least squares fits to the data are required that are still under development. So, in this study the radial component of the temperature tensor is used as a proxy for the actual temperature. We have searched for any dependence of the radial component of the temperature tensor upon the magnetic field direction, and have not found any significant relationship. This suggests that the distribution is fairly isotropic and that our proxy procedure is reasonable.

To investigate variations that depend upon things other than radial distance, it is necessary to remove radial variations as best possible. As the solar wind temperature at high latitudes is observed to scale approximately as r^{-1}, we scale temperature by a factor of r. Forty-eight hour averages of the temperature (radial component of the tensor) multiplied by r, distance from the Sun in AU, are shown in Fig. 8 for high latitude solar wind data with Northern hemisphere values being denoted by open boxes and Southern hemisphere values by open diamonds. Since radial gradients are larger than whatever latitudinal gradients might be present, to avoid biases the data were restricted to the same range of distances from the Sun to (1.55 to 3.03 AU). The data were fit to power laws; temperature was found to have a power law dependence of $r^{-1.03\pm0.03}$ in the Northern hemisphere and $r^{-0.81\pm0.02}$ in the Southern hemisphere. The formal uncertainties are calculated from a linear fit of $\log(T)$ as a function of $\log(r)$ with the power law index being the regression coefficient for the fit. The expression for the uncertainty in the regression coefficient (i.e., power law index) assuming a large number of samples, N, is given by (Udny-Yule and Kendall 1950) $\sigma_{\rm powerlawindex} = \sigma_{\log(T)}(1 - C^2)^{1/2}/(\sigma_{\log(r)}N^{1/2})$. Here, s denotes standard deviation, and C is the correlation coefficient between $\log(T)$ and $\log(r)$. The quoted uncertainties are obtained assuming that the 48 hour averages used were statistically independent. The power measured in the ecliptic of solar wind fluctuations below 10^{-6} Hz is typically flat; this corresponds to a sampling time of six days. Since our samples were two days length, an alternative estimate of the error in the slopes would be to multiply the above uncertainties by $3^{1/2}$, i.e., $r^{-1.03\pm0.05}$ in the Northern hemisphere and $r^{-0.81\pm0.03}$ in the Southern hemisphere. Within 2 AU Ulysses measured a higher temperature in the Northern hemisphere than in the Southern. Fig. 9 shows temperature as a function of solar wind speed for the high latitude; it may be noted that for equal temperatures, the plasma in the North is going about 1% faster than plasma in the South. To clarify the extent to which the velocity dependence accounts for the observed temperature differences, we fit the temperature to a linear function of solar wind speed, and used the relationship

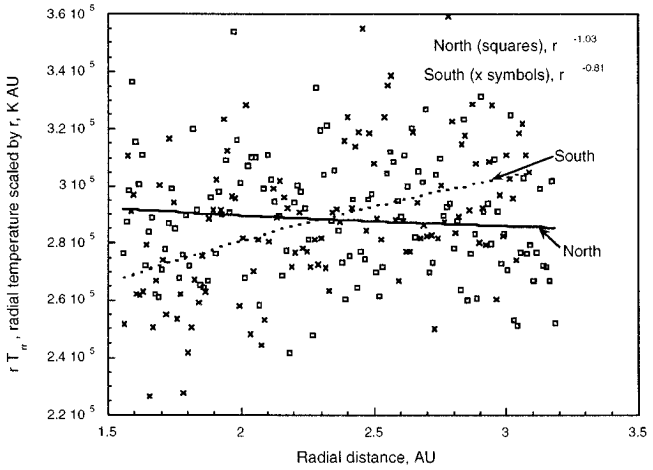

Fig. 8. Scaled radial temperature component

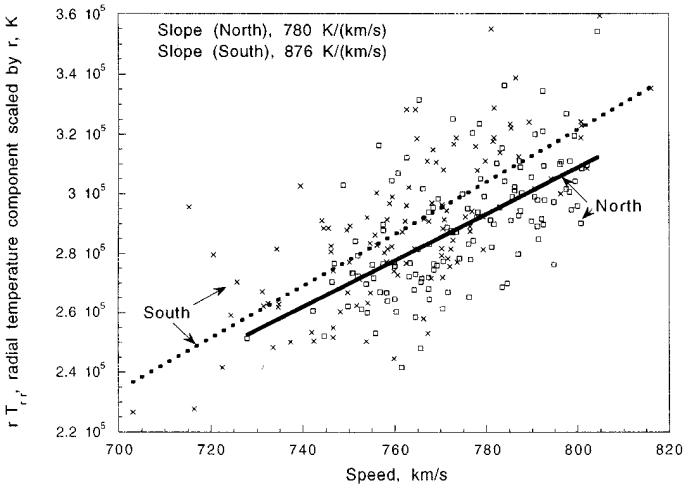

Fig. 9. rT_{rr} as function of solar wind speed, high latitude data only, symbol and line coding as in Fig. 8

between temperature and velocity to see if the temperature difference between the Northern and Southern hemispheres could be explained primarily in terms of a velocity difference. A plot (not shown) of the temperatures corrected for velocity similar to Fig. 8 resulted in the power law indices changing from -0.81 and -1.03 to -0.85 and -1.01. Correcting for the expected velocity dependence thus leaves the greater part of the differences between the two hemispheres unexplained.

It is also of interest to see whether the relationship that we obtained between velocity and temperature is in agreement with other work. Large scale compressions in the solar wind may affect the relationship between speed and temperature in the solar wind (Gosling et al. 1972); (Pizzo et al. 1973), and so we compare to Helios analyses (Lopez and Freeman 1986) as these are least likely to be subject to compressive effects and thus most directly comparable to Ulysses results. Lopez and Freeman investigated a number of choices as to functional relationships between velocity and temperature, and found that for velocities greater than 500 km/s best results were obtained with a linear relationship, whereas for lower velocities T is better estimated from the square of velocity (or perhaps the cube). Scaling the Helios temperatures by a power law in r to 1 AU, they find that for 1974 through 1976 (solar minimum) $T = 511V - 118400$, where T is temperature and V is solar wind speed, whereas we find $T = 872V + 216000$ for data in the range 700-850 km/s, and $503V - 95200$ using data in the range 500-850 km/s (fits not shown). This latter estimate is actually in very good agreement with that of Lopez and Freeman. However, if only the largest velocities are used, then T increases more rapidly with V than if lower velocities were included in the estimates. Lopez and Freeman investigated a number of function forms for fitting T as a function of V. We have scaled the Ulysses temperatures to 1 AU using a power law of $r^{-0.91}$ chosen as a compromise between the Northern and Southern hemisphere power laws. Fits to Ulysses data similar to those of Lopez and Freeman are shown in Table 1. Fits were done for the entire data set, all data with speeds >500 km/s, and all data with speeds <500 km/s. For the complete data set the number of averages was 310, and the standard deviation of the temperature before fitting was 5.4 10^4K. Comparable values for velocities greater (less) than 500 km/s are 280 (21) and 2.8 104 (4.2 10^4) K. Powers of 10 are denoted by integers following $\pm$ signs in the table. Two degrees of freedom were used when computing standard deviation of fitted data. For all the data, the exponential fit is worse than the linear fit at the 97% confidence level. The other fits are all statistically comparable. For high speed and low speed data considered separately, all functional forms work about as well as each other. Freeman and Lopez found that for low speed streams the linear fit was worst, and for high speed streams the exponential fit was worst. Ulysses is different than the in-ecliptic data, we believe, because most of the data is obtained at high latitudes and very high speeds, and this part of the data, which extends over a small range in velocity, contributes a large amount to the total fluctuations. In otherwords, we do not have enough data spaced over a wide range in velocity to say much about the functional form. Freeman and Lopez also found that for a linear fit of T to V in the slow speed wind the linear coefficient was 504 K/(km/s), and in the high speed wind the coefficient was 770 K/(km/s). Our results are 785 (slow wind), 410 (fast wind), and 503 (all data) K/(km/s). For the high latitude data only (a subset of the V> 500 km/s wind), we find 673 K/(km/s). This is less than the 780 (North high latitude) and 876 (South high latitude) indicated in Fig. 9. There is a statistical uncertainty of about 100 K/(km/s) in these estimates, and the remainder of the difference is probably due to the different power law in r used for temperature scaling (r^{-1} vs. $r^{-0.91}$) and combining (rather than keeping separate) the Northern and Southern data.

To determine what parameter, if any, does appear to be relatively well predicted by velocity, we considered expressions of the form $V = AT/(n^s r^t)$ where the power law indices s and t were chosen to obtain the best possible fit to V. On this basis, we find that $T/n^{1/2}$ is well predicted by velocity with good agreement between estimates obtained from the Northern and Southern hemispheres (Fig. 10). The radial dependencies

Table 1. Fits of T to V for various functional forms

Functional Form	Value of a	Value of b	Stnd. dev. of fits, K
All data:			
$aV+b$	503.	−1.14+5	2.37+4
$(aV+b^3$	0.050	26.2	2.48+4
$(aV+b)^2$	0.576	79.6	2.44+4
$(aV+b)^{3/2}$	5.85	−285.	2.42+4
aV^b	6.93	1.59	2.42+4
$a\exp(Vb)$	3.81+4	2.56−3	2.55+4
$V>500$ km/sec:			
$aV+b$	410.	−4.29+4	2.31+4
$(aV+b)^3$	0.035	37.9	2.32+4
$(aV+b)^2$	0.416	202.	2.32+4
$(aV+b)^{3/2}$	4.38	832.	2.32+4
aV^b	109.	1.18	2.31+4
$a\exp(Vb)$	7.54+4	1.67−3	2.32+4
$V<500$ km/sec:			
$aV+b$	785.	−2.34+5	2.5+4
$(aV+b)^3$	.129	−9.00	2.5+4
$(aV+b)^2$	1.31	−245.	2.5+4
$(aV+b)^{3/2}$	11.7	−2.87+3	2.5+4
aV^b	4.24−5	3.56	2.5+4
$a\exp(Vb)$	2.76+3	8.29−3	2.5+4

of $T/n^{1/2}$ (not shown) lead to power law indices of -1.06 for the Northern hemisphere and -0.76 for the Southern hemisphere.

6. Summary and discussion

The large scale properties of the solar wind observed during the fast latitude scan were as expected based on our previous observations of the solar wind in the ecliptic and the earlier Ulysses high latitude observations. During solar minimum, the current sheet is expected to lie close to the heliographic equator, and one would expect the slow speed solar wind to be confined to a narrow belt near the equatorial plane. This was in fact observed. As would be expected from the typically observed anticorrelation of density and velocity in the solar wind, number flux is observed to be one of the most well preserved constants in the solar wind. The average momentum flux in the equatorial region was about 20% lower than that at high latitudes, indicating the possibility that during solar minimum the heliopause would tend to have a longer extent in the poleward direction. North-South asymmetries of the solar wind were observed, with the higher speed Northern solar wind being associated with a smaller expansion factor as one might expect.

Useful quantitative information on the radial gradients of proton temperature were also obtained, and since these bear on the heating of the solar wind we discuss them further. Prior workers have investigated both the radial gradients of temperature, an indicator of the rate of internal dissipation in the solar wind, and also the relationship between velocity and temperature in the solar wind. Helios observations within 1 AU are well suited to comparison with Ulysses data, because shears and compression regions are less highly developed in the inner solar system than at 1 AU and beyond, and similarly these processes are not so important for Ulysses at high latitudes because of the lack of large scale velocity shears and compressions. The Helios observations also included the period of solar minimum. Determinations of radial gradients (Schwenn et al. 1981) using Helios 1 and Helios 2 lineups found that in high speed streams the plasma speed remained approximately constant and the temperature estimated using one dimensional energy spectra, i.e., the radial component of the temperature tensor, decreased with a power law estimated as $r^{-0.69}$ over the range 0.3 to 0.7 AU. In contrast, they found that in the low speed wind (up to 400 km/s) the temperature decreased as $r^{-1.21}$. For Helios in the inner solar system, the radial component of the temperature tensor is roughly equivalent to the parallel temperature. Using three dimensional temperature analyses, (Marsch et al. 1982) found that for solar wind speeds of 700-800 km/s, the parallel component of temperature decreased as $r^{-0.69}$ and the perpendicular component as $r^{-1.17}$. For a noncollisional model of the solar wind with adiabatic particle motion, if the interplanetary magnetic field were radial then the parallel temperature would be independent of radial distance and the perpendicular temperature would decrease as r^{-2}. The Helios results clearly indicate that a great deal of heating of the perpendicular component of the temperature was occurring because the $r^{-1.17}$ was considerably larger than r^{-2}, or taken together the net decrease was considerably less than the adiabatic value of -1.33.

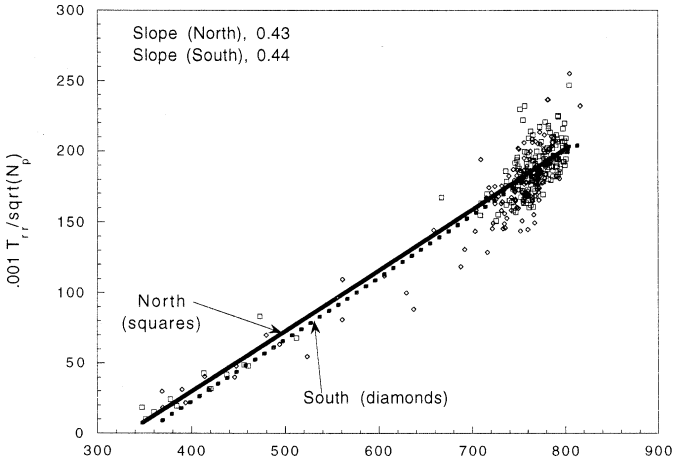

Fig. 10. $T_{rr}n^{-1/2}$ for high latitude and in-ecliptic data as a function of solar wind speed

In the case of the Ulysses data, $r^{-1.03}$ was found for the Northern hemisphere and $r^{-0.81}$ was found for the Southern hemisphere. By assuming the Parker spiral angle for the magnetic field, one can estimate the fraction of the contribution to the observed T_{rr} component of temperature from the parallel component of the pressure temperature; at 1.55 AU the contribution in the Northern (Southern) hemisphere is 0.83 (0.75), at 2.1 AU the contributions are 0.95 (0.95), at 2.8 AU are 0.65 (0.81), and at 3.05 AU are 0.51 (0.68). As the magnetic field

fluctuates considerably at higher latitude, it should not necessarily be assumed that the fractional contributions based upon the spiral angle are realistic. We have searched for a dependence of T_{rr} upon the observed magnetic field direction, and although some methods of selecting data and comparing data do show some weak correlations, no correlations of sufficient magnitude to explain the difference between the North and South temperature gradients are readily apparent. If Ulysses is observing primarily the parallel component of temperature, then the Ulysses temperature decrease is a steeper power law than observed in the parallel component of the Helios temperature. Alternatively, if Ulysses observations reflect a mixture of parallel and perpendicular components, then the temperature decrease is probably roughly comparable to that obtained by combining the Helios parallel and perpendicular temperature gradient observations. A possible explanation of our failure to find strong correlations with magnetic field direction is that the temperature at high latitudes is not too far from isotropic; however, some MHD scale correlation between magnetic field direction and temperature in the solar wind might also affect the observations.

As turbulence in the solar wind evolves, wave heating should be less intense at greater distances in the solar system (Tu 1988). Goldstein et al. (1995) have compared Helios and Ulysses turbulence measurements and find that the turbulence is most evolved as seen by Ulysses at 4 AU, is less evolved at 2 AU, and is least of all evolved as seen at Helios. As a less evolved turbulence has more energy available to heat the plasma, a steeper radial gradient of temperature seen at Ulysses than at Helios might be expected, and this is a possible interpretation of the data. Quantitative verification of this possibility requires a better assessment of the relative parallel and perpendicular temperature components, and estimate of the actual heating rate from the radial evolution of magnetic field power spectra.

We can also compare our temperature gradients with those reported in the ecliptic from previous observers. From Pioneer 10 and 11 data a power law of $r^{-0.7}$ was found over distances from 1 to 9 AU (Smith and Wolfe 1979). Gazis (1984) using Voyager 1 data found a power law behavior of roughly about $r^{-0.8}$ for plasma with velocities in the range 500 to 800 km/s over distances from 1 to 10 AU. Liu et al. (1995) using Ulysses SWICS ion mass spectrometer data over the range 1.5 to 5 AU found for velocities greater than 500 km/s a dependence of $r^{-0.95}$, approximately in the same range of values as we find at high latitude (the average of -0.81 (South) and -1.03 (North) is -0.92). These numbers are in general a bit less steep with radial distance than the Ulysses numbers, but heating from stream interactions and shocks may be affecting these in-ecliptic observations. There are further obvious comparison difficulties. For example, as is apparent in Fig. 4, there is a large gradient in the momentum flux observed by Ulysses during the time period of the Liu et al. study, and this study did not use measurements at 1 AU as a baseline. Liu et al. also estimated the radial gradient of density for high speed streams during this time and found a $r^{-1.36}$ relationship; this could be attributed either to the high speed streams colliding with low speed streams or a time evolution of the solar wind as Ulysses increased its distance from the Sun. Summarizing the temperature results, things are much as expected with the biggest surprise (currently not understood) being the different radial temperature gradients in the Northern and Southern hemispheres.

Acknowledgements. This paper presents the results of one phase of research conducted at the Jet Propulsion Laboratory, California Institute of Technology, under contract with the National Aeronautics and Space Administration (NASA). The work at the Los Alamos National Laboratory was performed under the auspices of the U. S. Department of Energy with financial support from the NASA under W-15847.

References

Bame, S.J., McComas, D.J., Barraclough, B.L., Phillips, J.L., Sofaly, K.J., Chavez, J.C., Goldstein, B.E., Sakurai, R.K.: 1992, Astron. and Astrophys. Suppl. 92, 237

Feynman, J., Spitale, G., Wang, J., Gabriel, S. 1993, J. Geophys. Res. 98, 13281

Gazis, P.R. 1984, J. Geophys. Res. 89, 775

Goldstein, B.E., Smith, E.J., Balogh, A., Horbury, T.S., Goldstein, M.L., Roberts, D.A. 1995, Geophys. Res. Lett. 22, 3393

Gosling, J.T., Bame, S.J., Feldman, W.C., McComas, D.J., Phillips, J.L., Goldstein, B., Neugebauer, M., Burkepile, J., Hundhausen, A.J., Acton, L. 1995, Geophys. Res. Lett. 22, 3329

Gosling, J.T., Feldman, W.C., McComas, D.J., Phillips, J.L., Pizzo, V.J., Forsyth, R.I. 1995, Geophys. Res. Lett. 22, 3333

Gosling, J.T., Hundhausen, A.J., Pizzo, V., Asbridge, J.R. 1972, J. Geophys. Res. 77, 5442

Lazarus, A.J., McNutt, R.L.J. 1990, Physics of the Outer Heliosphere 229-234

Liu, S., Marsch, E., Livi, S., Woch, J., Wilken, B., von Steiger, R., Gloeckler, G. 1995, Geophys. Res. Lett. 22, 2445

Lopez, R.E., Freeman, J.W. 1986, J. Geophys. Res. 91, 1701

Marsch, E., Mhlhuser, K.-H., Schwenn, R., Rosenbauer, H., Pilipp, W., Neubauer, F.M. 1982, J. Geophys. Res. 87, 52

Neugebauer, M., Snyder, C.W. 1966, J. Geophys. Res 71, 4469

Phillips, J.L., Bame, S.J., Barnes, A., Barraclough, B.L., Feldman, W.C., Goldstein, B.E., Gosling, J.T., Hoogeveen, G.W., McComas, D.J., Neugebauer, M., Suess, S.T. 1995, Geophys. Res. Lett. 22, 3301

Pizzo, J., Gosling, J.T., Hundhausen, A.J., Bame, S.J. 1973, J. Geophys. Res. 78, 6469

Schatten, K.H. 1971, Cosmic Electrodynamics 2, 232

Schwenn, R. 1990, Physics of the Inner Heliosphere. 1. Large-Scale Phenomena 99

Schwenn, R., Mhlhuser, K.-H., Marsch, E., Rosenbauer, H. 1981, Solar Wind Four 126

Smith, E. J., Balogh, A., Burton, M. E., Erdos, G. E. O. S., Forsyth, R. J. 1995, Geophys. Res. Lett. 22, 3325

Smith, E.J., Wolfe, J.H. 1979, Space Sci. Rev. 23, 217

Strong, J.B., Asbridge, J.R., Bame, S.J., Heckman, H.H., Hundhausen, A.J. 1966, Phys. Rev. Letts. 16, 631

Tu, C.-Y. 1988, Proceedings of the Sixth International Solar Wind Conference 2, 593

Udny-Yule, G., Kendall, M.G. An Introduction to the Theory of Statistics, Charles Griffin, London, 1950

Wang, Y.-M., Hawley, S.H., Sheeley, N.R.J. 1996, Science 271, 464-469

Wang, Y.-M., Sheeley, N.R., Jr. 1988, J. Geophys. Res. 93, 11227

Wang, Y.-M., Sheeley, N.R., Jr. 1990, Astrophys. J. 355, 726